Available online at www.sciencedirect.com
ScienceDirect
Journal of Photochemistry and Photobiology A: Chemistry 196 (2008) 1–9
Journal of Photochemistry and Photobiology A:Chemistry
www.elsevier.com/locate/jphotochem

Solid-state photochemistry of dirhenium carboxylates and the deposition of rhenium oxide thin films

Juan Pablo Bravo-Vasquez *, Ross H. Hill

Simon Fraser University, Burnaby, BC V5A 1S6, Canada

Received 23 July 2007; received in revised form 2 November 2007; accepted 10 November 2007
Available online 19 November 2007

Abstract

Rhenium carboxylates of general formula $Re_2(O_2C_nH_{2n+1})Cl_2$ where $n = 5$–8, were studied as precursors for the photochemical deposition of rhenium trioxide thin films. Solutions of the inorganic complexes were spin coated on p-type silicon(1 0 0) substrates and the solid-state photochemistry studied at room temperature. These compounds were deposited by spin coating onto silicon(1 0 0) forming crystalline thin films with lamellar, bilayers structures with planes of rhenium(III) coordinated to the carboxylate group as demonstrated by X-ray diffraction experiments. The carboxylates complexes underwent a photochemical reaction, consistent with the decarboxylation of carboxylate ligand to generate CO_2 and the radical disproportionation products. The photolyzed films showed sensitivity towards atmospheric water, transforming into a rhenium bronze structure of the type H_xReO_3. Auger electron spectroscopy indicated that the final film is carbon free and composed only of Re and O. The same behavior was observed in all the rhenium carboxylates independent of the alkyl chain length. The 2-ethylhexanoate complex did form amorphous thin films which also show the highest quantum yield ($\Phi = 0.004$).

Keywords: Rhenium oxide; Photochemistry; Thin films; Rhenium(III) carboxylates

1. Introduction

Rhenium metal and its oxides have attracted interest for applications in a variety of areas, with the most common being catalysis [1,2]. Lately, interest in metals and metal oxides has increased in applications like gate electrodes and buffer layers in electronic devices [3]. Buffer layers are required to reduce the electron-migration of the materials in integrated circuits under electrical bias. They have also being applied in superconducting thin films, preventing the direct interaction of the superconductor with the substrate materials [4]. ReO_3 is a good candidate as thin film for application as buffer layer because of its low resistivity, thermal stability and good oxidation resistance [5].

ReO_3 structure is the simplest framework structure for an MX_3 compound [6]. Its structure is based on six coordinate pseudo-octahedral Re(VI) building blocks, with the octahedral units connected in a corner-sharing fashion forming a 3D network [7]. Rhenium trioxide is also attractive since it is a conductor oxide [8] with the conductivity arising from partially filled 4d states and the mixing of metal and oxygen atomic orbitals.

Thin films of ReO_3 have been deposited by methods like smoked evaporation of the metal oxide [9], RF magnetron sputtering, [5] and dc magnetron sputtering [10]. However, sputtering methods lack control over the oxidation process, often forming Re_2O_7 as a by-product. Re_2O_7 can also vaporize due to its high vapor pressure at the conditions of deposition. Hence, room temperature fabrication would appear to be an optimal approach for the deposition of rhenium oxide thin films. We have being working on approaches to the deposition of metal oxide thin films involving the use of amorphous thin film from an inorganic precursor, and later decomposed the complex using some energy source, like UV light [11]. The method relies in that the light induces a photochemical reaction, which triggers the decomposition of the starting material.

In this paper we present our studies regarding the photoreactivity of molecular dirhenium complexes with carboxylic acids on silicon surfaces. The carboxylate complexes selected for this

* Corresponding author. Current address: National Institute for Nanotechnology, Edmonton, Alberta T6G 2M9, Canada. Tel.: +1 780 6411754; fax: +1 780 641 1601.
E-mail address: juan-pablo.bravo-vasquez@nrc-cnrc.gc.ca (J.P. Bravo-Vasquez).

1010-6030/$ – see front matter © 2007 Elsevier B.V. All rights reserved.
doi:10.1016/j.jphotochem.2007.11.006

study were the rhenium(III) carboxylates of general formula $Re_2(O_2C_nH_{2n-1})_4Cl_2$, where n ranged between 5 and 7. This complexes showed interesting behavior when spin coated on surfaces, self-assembling and forming highly organized layered structures. Solutions of rhenium carboxylate were spin coated on silicon to form optical quality thin films and their photochemistry was studied at 254 nm wavelength. Our results show that all the complexes decomposed when exposed to the UV light and that rhenium trioxide is form upon photolysis. A secondary reaction was observed on photolyzed thin films in which the ReO_3 transform into a rhenium bronze (H_xReO_3) structure.

2. Experimental

2.1. Materials and instruments

All solvents and reagents were purchased from Aldrich and used without further purification unless specifically stated. The p-type Si(1 0 0) wafers used in this study were purchased from Pacific Microelectronic Center, Canada. The wafers were cut to the approximate dimensions of 10 mm by 15 mm in our laboratory. CaF_2 discs were obtained from Wilmad Glass Co. Inc., FTIR spectra were obtained using a Bomem–Michelson 120 FTIR spectrometer. Electronic absorption spectra were obtained in the range from 190 to 800 nm using a Hewlett Packard HP8452A photodiode array spectrophotometer. Auger electron spectra were obtained using a PHI double pass cylindrical mirror analyzer (CMA) at 1 eV resolution. Films thickness was determined using a Leitz Laborlux 12MES optical microscope with a Michelson interference attachment. The irradiation source was a 254 nm low pressure Hg lamp from Orion, Co. Cut off filters and a water filter were used to remove unwanted wavelengths and thermal effects, respectively. X-ray diffraction spectra were obtained using a Phillips X-ray diffractometer operating at 35 KV and 45 A. The X-ray source was monochromatic Cu Kα (1.54 A) line. The experiment resolution was 0.05°.

2.2. Synthesis of rhenium carboxylates

The synthesis of the acetate and pentanoate complexes was performed according to literature procedures [12]. A modification of the published method was used in the synthesis of the complexes with 2-ethylhexanoic, hexanoic and heptanoic acid. In this modification, the rhenium(III) acetate was suspended in the minimum amount of the corresponding degassed carboxylic acid and the mixture was heated. After a couple of minutes the solution turns red once the acetate had dissolved. The solution was then heated for 8 h under nitrogen. Addition of hexane and cooling of the solution precipitated the corresponding carboxylate product.

2.3. Thin film deposition

Optical quality thin films of rhenium(III) carboxylates were formed on the substrates by spin coating. Chloroform solutions of the respective rhenium(III) carboxylate (10% w/w) were filtered through 0.25 μm to removed insoluble particulates prior to spin coating. The solution was then dispensed onto a silicon chip and the substrate spanned at 300 rpm for 20 s.

2.4. Calibration of absorption on surface

A stock solution of rhenium(III) pentanoate (0.0024 g) was prepared in $CHCl_3$ (5 ml). A drop (3.3 μl) of this solution was then deposited on the surface of a silicon chip using a microsyringe. The solvent was allowed to evaporate and the FTIR spectrum was obtained. The spectrum corresponds to a concentration of 2.4×10^{-9} mol cm^{-2} (area = 0.785 cm^2). This process was repeated several times and the calibration curve of absorbance versus concentration (mol cm^{-2}) was constructed. The slope of this graph corresponds to the infrared extinction coefficient (ε_{IR}), which was found to be 1.16×10^6 mol^{-1} cm^2. The extinction coefficients for the other absorption bands were obtained relative to the absorption at 1460 cm^{-1}. The same procedure was followed to determine the infrared extinction coefficient of the absorption bands in the infrared of all the other complexes studied. The extinction coefficients at the wavelength of photolysis (254 nm) were obtained as follows: a sample of rhenium(III) pentanoate was spin coated onto CaF_2 optical flats. Both FTIR and UV–vis spectra were obtained for the sample. The ratio of the absorbance, A_{UV} at 254 nm, to the absorbance, A_{IR} at 1460 cm^{-1}, was 6.182. This ratio was multiplied by the extinction coefficient in the infrared, ε_{IR}, in units of cm^2 mol^{-1} yielding an extinction coefficient (ε_{UV}) at 254 nm of 7.67×10^6 mol^{-1} cm^2.

2.5. Photolysis

All photolysis experiments were done in the same manner. Spin coating on the surface of a silicon chip formed a rhenium(III) carboxylate thin film. The chip was clamped to the sample holder inside a chamber. A dry atmosphere was kept inside the chamber by flowing air that was previously dried through Drierite and an acetone/dry ice trap. An FTIR spectrum was measured though CaF_2 windows and then the film was irradiated for 5 min with 254 nm light. As stated above, water filter was used to remove unwanted thermal effects. A second FTIR spectrum was then measured. This procedure was repeated several times until complete reaction (no IR bands of starting material).

3. Results

Optical quality thin films of rhenium(III) carboxylates were formed on the substrates by spin coating. This was accomplished by the delivery of a chloroform solution of the complex onto a spinning silicon chip. The solvent evaporates and a thin film is formed on the substrate. Chloroform was chosen as solvent, because it rendered the best quality thin films (compared to other solvents tested such as dichloromethane, ketones, methanol, etc.). Polar protic solvents like methanol deposited powdery thin films. This can be explained by the dissociation of the carboxylate complex when dissolved in alcohol.

Table 1
FTIR spectroscopic data for the rhenium(III) complexes

Complexes	Wavenumber , cm^{-1}, (ε_{IR}, mol^{-1} cm^2)[a]	Assignment [23,24]
$Re_2(O_2C_5H_9)_4Cl_2$	1460 (1.00)	$\delta_s(CH_3)$
	1440 (0.73)	$\nu_a(CO_2)A_{2u}$
	1418 (0.72)	$\delta_s(CH_3)$
	1296 (0.28)	$\nu_s(CO_2)E_u$
$Re_2(O_2C_6H_{11})_4Cl_2$	1458 (0.98)	$\delta_s(CH_3)$
	1437 (0.95)	$\nu_a(CO_2)A_{2u}$
	1419 (0.98)	$\delta_s(CH_3)$
	1402 (0.33)	$\delta_s(CH_3)$
	1310 (0.12)	$\nu_s(CO_2)E_u$
$Re_2(O_2C_7H_{13})_4Cl_2$	1463 (0.67)	$\delta_s(CH_3)$[c]
	1441 (0.96)	$\nu_a(CO_2)A_{2u}$
	1432 (0.72)	$\delta_s(CH_3)$
	1390 (0.40)	$\delta_s(CH_3)$[c]
	1321 (0.24)	$\nu_s(CO_2)E_u$
$Re_2(O_2C_8H_{15})_4Cl_2$	1462 (1.11)	$\delta_s(CH_3)$[c]
	1424 (1.82)	$\nu_a(CO_2)A_{2u}$
	1321 (0.78)	$\nu_s(CO_2)E_u$

[a] Instrument uncertainty 0.05°.

The thin films of rhenium(III) carboxylates were characterized by transmission FTIR, UV–vis and X-ray diffraction spectroscopies. Unless specifically stated, a silicon chip was used as the substrate. Oxide coated silicon was used in the X-ray diffraction experiments and CaF_2 optical flats were used for UV–vis spectroscopy studies.

3.1. FTIR spectroscopy of rhenium(III) carboxylates

A thin film of rhenium(III) pentanoate deposited on silicon(1 0 0) was analyzed by FTIR (Table 1). Apparent in the spectrum are five absorption bands in the range 1460–1290 cm^{-1}. Three of them dominate the spectrum and are due to the carbonyl and alkyl groups in the carboxylate ligand. The antisymmetric (A_{2u}) and symmetric (E_u) CO_2 stretches are assigned to the absorption bands at 1440 and 1296 cm^{-1}, respectively. The difference between the antisymmetric and symmetric stretches ($\Delta\bar{\nu}$) has been used to distinguish the types of bonding of carboxylates with metals. The $\Delta\bar{\nu}$ value is known to decrease in the order: unidentate > ionic > bridging > bidentate.

The $\Delta\bar{\nu} = 144\ cm^{-1}$ of rhenium(III) pentanoate agrees with the value for a bridging carboxylate group. It is also consistent with the crystal structure of the acetato derivative [13]. Therefore, this carboxylate bridge is a syn–syn type, which allows the direct interaction of the two-rhenium atoms in the molecule.

The FTIR also shows two intense bands at 1460 and 1418 cm^{-1}. The alkyl chain of the carboxylate ligand is known to have bands associated with the CH_3/CH_2 bending modes at about 1400 cm^{-1}. There is presumably a significant mixing between the vibrational modes of the antisymmetric CO_2 stretch and the alkyl group deformation stretch which could explain the stronger than expected intensity in the alkyl group absorption band.

The FTIR spectroscopic data for thin films of the other rhenium(III) carboxylate complexes is also presented in Table 1. The spectral data of the other complexes did not differ significantly from the rhenium(III) pentanoate data. In each case, one intense band and one weak band are found associated with the antisymmetric and symmetric modes of the carboxylate group, respectively. In general, the symmetric stretch appears weaker in the spectra. Additional band(s) associated with the alkyl group deformation are also present. As previously mentioned, an increase in the intensity of the band was observed when going from C_3 to C_8.

3.2. Electronic spectroscopy of rhenium(III) carboxylates

The solid-state electronic spectra of the rhenium(III) carboxylates were determined by UV–vis spectroscopy. Optical quality thin films of rhenium(III) pentanoate and the other complexes were spin coated on CaF_2 optical flats.

The spectrum is dominated by two intense absorptions at 214 and 276 nm. The band at 276 nm was previously assigned to the charge transfer transition $\pi(Cl) \rightarrow \delta^*(Re)$ by Cotton et al. They reported that the wavelength of the absorption changed remarkably when the halogen ligand is exchanged, but it was unaffected by changes in the carboxylate ligand. The absorption at ~214 nm can be assigned to intraligand electronic transitions of the carbonyl group. Carboxylate groups tend to show $\pi \rightarrow \pi^*$ and $n \rightarrow \pi$ transitions in the region 190–210 nm, which should shift to longer wavelength upon coordination.

In the visible region of the spectrum, bands at approximately 482 and 500 nm are expected for rhenium(III) carboxylates. These transitions were not observed in our solid-state spectrum. These expected absorptions are the electric-dipole forbidden but vibronically allowed $\pi(Re) \rightarrow \delta^*(Re)$ ($^1A_{1g}$–^3E_g) and the electronically allowed $\delta(Re) \rightarrow \delta^*(Re)$ ($^1A_{1g}$–$^1A_{2u}$) transitions, respectively [14]. Although the later transition is allowed, it is not sufficiently intense to be observed in these films.

The electronic absorption spectra for the complexes are summarized in Table 2. The spectra of all the complexes show similar features: intense charge transfer absorption at 274 ± 4 nm due to the $\pi(Cl) \rightarrow$ Re transition and a shorter wavelength band associated with the carboxylate ligand. The weak *d–d* transitions were not observed in the solid-state spectrum.

Table 2
Electronic absorption data for the rhenium(III) carboxylates

Complexes	Wavelength, nm (ε_{UV}, mol^{-1} cm^2)	Assignment [25]
$Re_2(O_2C_5H_9)_4Cl_2$	216 (1.92)	
	276 (1.69)	$\pi(Cl) \rightarrow \delta^*(Re)$ ($^1A_{1g} - {}^1E_u$)
$Re_2(O_2C_6H_{11})_4Cl_2$	214 (1.75)	
	274 (1.42)	$\pi(Cl) \rightarrow \delta^*(Re)$ ($^1A_{1g} - {}^1E_u$)
$Re_2(O_2C_7H_{13})_4Cl_2$	214 (2.10)	
	278 (2.02)	$\pi(Cl) \rightarrow \delta^*(Re)$ ($^1A_{1g} - {}^1E_u$)
$Re_2(O_2C_8H_{15})_4Cl_2$	214 (2.28)	
	282 (2.37)	$\pi(Cl) \rightarrow \delta^*(Re)$ ($^1A_{1g} - {}^1E_u$)

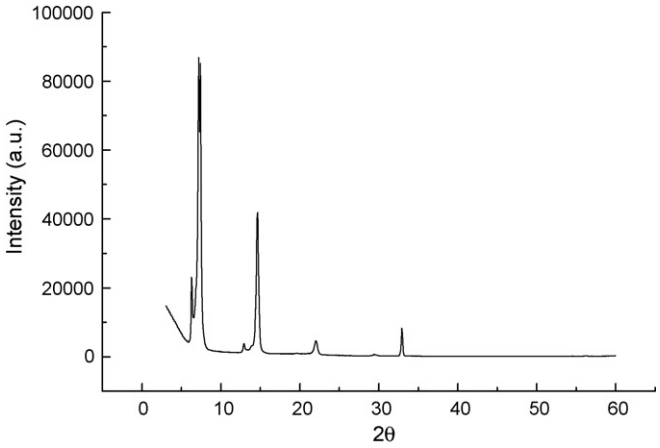

Fig. 1. X-ray diffraction of thin film of rhenium(III) pentanoate on silicon oxide wafer.

3.3. X-ray diffraction

Thin films of the rhenium(III) carboxylates deposited on oxide-coated silicon were investigated by X-ray diffraction. A thin film of rhenium(III) pentanoate was mounted on a glass slide and the X-ray diffraction pattern was obtained using monochromatic Cu Kα radiation (λ = 1.54 Å). The X-ray diffraction pattern of rhenium(III) pentanoate is presented in Fig. 1. The thin film of rhenium(III) pentanoate produced a well-defined X-ray spectrum. The X-ray pattern contains a series of sharp equidistant Bragg reflections, indicative of at least one-dimensional order in the film of rhenium(III) pentanoate. The pattern consists of reflections at 2θ of approximately 8°, 15° and 22°. Indexing of the X-ray diffraction pattern indicates that the observed reflections correspond to the successive (0 0 *l*) reflections planes of an ordered system consistent with a lamella structure with a interlayer spacing of 12 Å. A second family of reflections at 2θ of 4.4°, 8.9° and 15.3° is observed in some cases, corresponding to a d spacing of approximately 20 Å. This is consistent with patterns resulting from a tetragonal distortion of the alkyl chain arrangement and it is dependent on the deposition conditions.

The remaining long chain complexes show similar X-ray diffraction patterns. Films of rhenium(III) hexanoate and rhenium(III) heptanoate show the diffraction peaks corresponding to the (0 0 *l*) reflections,. Similarly to the rhenium pentanoate, a second family of reflections, significantly less intense than the main reflection, is sometimes observed. The X-ray diffraction peaks for all the complexes are summarized in Table 3. From the XRD data, the interlayer spacing calculated for thin films of rhenium(III) hexanoate and heptanoate are 15 and 16 Å, respectively.

Table 3
X-ray diffraction angles for rhenium(III) carboxylate on oxide coated silicon

Complexes	2θ value[a]	*d* spacing[b]
$Re_2(O_2C_5H_9)_4Cl_2$	7.61 (100), 14.8 (27), 22.5 (5)	11.8
$Re_2(O_2C_6H_{11})_4Cl_2$	5.85 (100), 11.6 (34), 17.6 (13)	15.1
$Re_2(O_2C_7H_{13})_4Cl_2$	5.31 (100), 10.50 (29), 17.62 (11)	16.2
$Re_2(O_2C_8H_{15})_4Cl_2$		

[a] Instrument uncertainty 0.05°.
[b] Average value in Å.

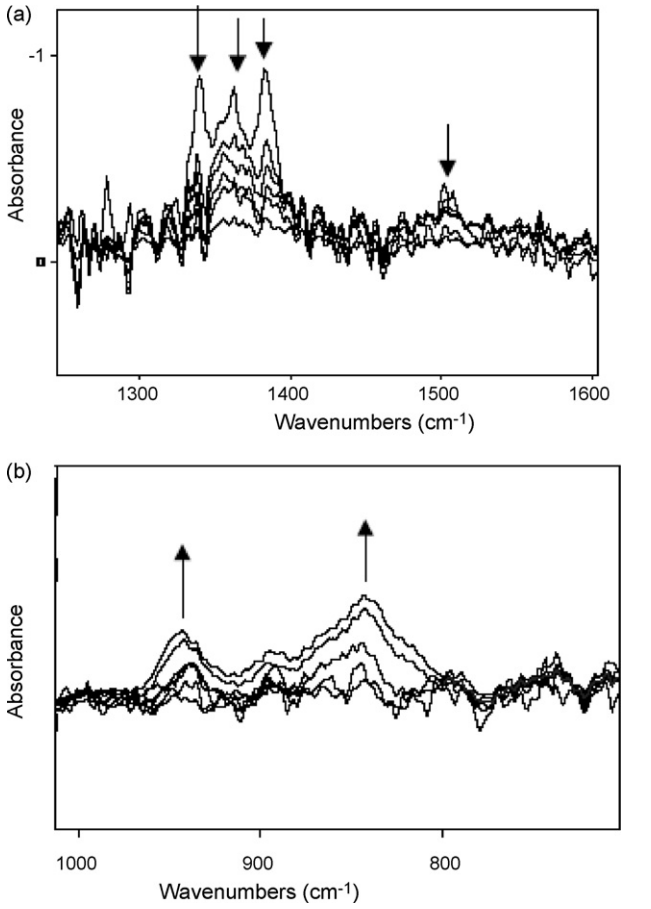

Fig. 2. FTIR spectral changes in the metal carboxylate (top) and metal oxide (bottom) regions for the photolysis of a film of rhenium(III) pentanoate. Times of photolysis are 0, 22, 35, 68, 84 and 156 min.

The 2-ethylhexanoate complex did not show any peaks in the X-ray spectrum, indicative of the amorphous nature of the precursor thin film. The presence of the side chain in the carboxylate ligand may disturb the self-alignment of the carboxylate molecules preventing the formation of a lamellar structure.

3.4. Photolysis

A thin film of rhenium(III) pentanoate was placed in a photolysis chamber as previously described. Vibration bands due to the antisymmetric and symmetric carboxylate were observed at 1440 and 1296 cm^{-1}, respectively. Vibration bands from the alkyl groups at 1460 and 1418 cm^{-1} were also evident. The sample was exposed to 254 nm light for 22 min and the FTIR was measured. Fig. 2 illustrates the spectral changes in the carboxylate region observed during the photolysis of the film of rhenium(III) pentanoate. After 22 min of photolysis, the carboxylate bands at 1440 and 1296 cm^{-1} had decreased by approximately 50%. No new vibration bands in the 1500–1200 cm^{-1} range were observed. In addition, the vibration bands at 1460 and 1418 cm^{-1}, attributed to the CH_2 group in the alkyl chain, decreased in intensity. This indicated that

Table 4
FTIR absorption bands of photolyzed thin films in dry air

Complexes	Vibration bands	Assignment
$Re_2(O_2C_5H_{11})_4Cl_2$	943	$\nu_{as}(ReO_3)$
	845	ν_{as}(O–Re–O)
$Re_2(O_2C_6H_{13})_4Cl_2$	939	$\nu_{as}(ReO_3)$
	851	ν_{as}(O–Re–O)
$Re_2(O_2C_7H_{15})_4Cl_2$	941	$\nu_{as}(ReO_3)$
	845	ν_{as}(O–Re–O)
$Re_2(O_2C_8H_{17})_4Cl_2$	941	$\nu_{as}(ReO_3)$
	847	ν_{as}(O–Re–O)

Instrument resolution $\pm 4\,cm^{-1}$.

the carboxylate ligand is lost upon photolysis. Careful examination of the 1000–800 cm^{-1} region in the FTIR showed the growth of two broad bands centered at 943 and 845 cm^{-1}. These absorptions were assigned as the $\nu_{as}(ReO_3)$ and ν_{as}(O–Re–O) absorptions, respectively and they agreed with published results [15]. A similar trend was observed when the reaction was monitored longer times; with the absorption bands of the carboxylate ligands decreasing until no sign of remaining ligand could be detected in the film. In the oxide region of the spectrum, the two absorptions from the oxide product were clearly evident.

After extensive photolysis, no evidence for absorption bands other than the oxide was found. The bands associated with the starting material, $Re_2(O_2C_5H_9)_4Cl_2$, were no longer observable. The other rhenium(III) carboxylates were also cast as thin films and exposed to 254 nm light at room temperature. In each case, the vibration bands in the range of 1500–1290 cm^{-1}, corresponding to the carboxylate ligands (symmetric, antisymmetric and alkyl deformation bands), decreased in intensity without growth of new bands in the indicated range. Also, the vibration bands associated with rhenium oxygen bonds were observed to grow in the range of 950–840 cm^{-1}. The FTIR absorption bands found in the films after photolysis are summarized in Table 4. In all cases, the two absorption bands centered at approximately 940 and 840 cm^{-1} are the only absorption bands detected after photolysis. These absorptions were assigned as the $\nu_{as}(ReO_3)$ and ν_{as}(O–Re–O) of rhenium oxide. After the sample has been left in the air for several hours, it was evident that the photolyzed film suffers changes. The two bands originally observed after photolysis in dry air coalesce into a single sharp band centered at $902 \pm 1\,cm^{-1}$. This peak was found in all the samples after photolysis and exposed to ambient air. The peak is strongly resembling of the FTIR of evaporated ReO_3 on silicon described by Ishii et al. [9].

4. Mass spectroscopy of the volatile organic photoproducts

Mass spectroscopy was used to identify the volatile products from the photolysis of the rhenium(III) carboxylates. A thin film of rhenium(III) pentanoate was placed inside a sealed quartz cell and photolyzed for 3 h. After exposure, the chamber was connected to a mass spectrometer for analysis of the gaseous products. The spectrum showed the signals consistent with the fragmentation of the starting material. The highest intensity peaks observed correspond to CO_2 (m/z of 44) and H_2O (m/z of 18). For m/z higher than 44, the spectrum showed two families of peaks at 27, 41, 56 and 29, 43, 58. These families are consistent with fragmentation patterns due to C_4H_8 and C_4H_{10}, respectively. Thus, the mass spectrum is consistent with products from a decarboxylation reaction of the pentanoate ligand. After photon absorption, the carboxylate group will lose CO_2, (detected in the MS) and produce an alkyl radical fragment, $[C_4H_9]^{\bullet}$. Later, this radical can disproportionate to yield C_4H_{10}($m/z = 58$) and C_4H_8($m/z = 56$), both molecular ions detected in the MS, by hydrogen abstraction. Similar results were obtained from the photolysis experiment of the other carboxylate complexes on silicon. For example, the mass spectrum obtained from a sample of 2-ethylhexanoate complex showed a fragmentation peak at m/z of 44 and two other sets of peak families. The first set was found at m/z 41, 56, 69 and 98. These peaks are consistent with the fragmentation pattern of 3-heptene (C_7H_{14}). The second family of peaks was found at m/z values of 43, 57, 71 and 100. This pattern is consistent with heptane (C_7H_{16}). Again, these products, heptane and 3-heptene, can be formed from the disproportionation reaction of the decarboxylation product, $[C_7H_{15}]^{\bullet}$, of the 2-ethylhexanoate ligand. Therefore, mass spectrometry indicates that the major volatile products of the photolysis of rhenium(III) carboxylate complexes are the products of the decarboxylation of the carboxylate ligands, CO_2 and radical disproportionation products.

4.1. X-ray diffraction of photolyzed thin films

Samples of photolyzed thin films of rhenium(III) pentanoate were analyzed by powder X-ray diffraction (Fig. 3). After photolysis, the X-ray spectrum showed three reflections at 16.4°, 25.4° and 51.3°. These reflections are consistent with the (1 1 0), (2 1 0) and the (3 3 0) planes of a hexagonal ReO_3 phase with approximately lattice parameter $a = 4.72$ and $c = 4.36$, respectively [16]. When the thin film produced from rhenium(III) pentanoate were left in air for longer periods of time (>70 h), the initially smooth film became powdery. The diffraction pattern

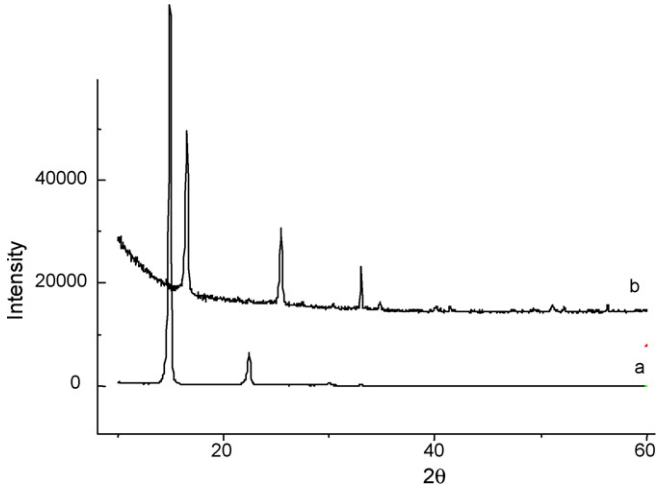

Fig. 3. XRD spectra of rhenium(III) pentanoate deposited on oxide coated silicon, (a) before and (b) after 40 h of photolysis.

Table 5
X-ray diffraction data for the photolyzed thin films of rhenium(III) carboxylates and ReO_3 and H_xReO_3 literature[a]

Complex	2θ angle (°)	hkl index	2θ ReO_3 (°)	2θ H_xReO_3 (°)
$Re_2(O_2C_5H_9)_4Cl_2$	16.43	110	16.56	16.36
	25.52	210	25.5	25.45
	51.30	330	51.07	50.90
$Re_2(O_2C_6H_{11})_4Cl_2$	16.53	110	16.56	16.36
	25.46	210	25.5	25.45
	56.25	006	56.78	56.82
$Re_2(O_2C_7H_{13})_4Cl_2$	16.70	110	16.56	16.36
	25.33	210	25.5	25.45
	56.30	006	56.78	56.82

[a] Time: 70 h in air.

showed the appearance of more reflections at 2θ angles of 16.8° (1 1 0), 25.7° (1 2 1), 30.7° (2 0 0), 33.8°(2 1 1), 41.8°(2 4 0), 47.1° (1 6 1) and 51.4° (1 7 0). These changes in the X-ray diffraction pattern of ReO_3 when left in air are consistent with previous reports that indicated the formation of a rhenium bronze (H_xReO_3) [17]. The Bragg diffractions for a polycrystalline sample of H_xReO_3 had been reported at approximate 2θ angles of 16.4°, 25.45°, 27.7°, 30.2°, 34.8°, 41.1° and 50.9°. This behavior of ReO_3 can be explained by the reactivity of ReO_3 towards water vapor and can be represented by the following chemical equation:

$$(1 + x)ReO_3 + xH_2O \rightarrow H_xReO_3 + HReO_4 \quad (1)$$

The oxide films produced from the other rhenium(III) carboxylates also showed a similar behavior. After 40 h of photolysis, the initial peaks had disappeared and three other diffraction peaks grew in intensity. All the other photolyzed thin films made of rhenium(III) carboxylates only showed two diffraction peaks at 2θ angles of approximately 16° and 25° in their X-ray pattern and a third one at ∼50° later in the photolysis. The final Bragg reflections for the photolyzed thin films are summarized in Table 5.

Photolyzed thin films of rhenium(III) 2-ethylhexanoate showed only a single diffuse Bragg reflection centered at a 2θ angle of approximately 20°. This indicates that the thin film before and after photolysis is amorphous.

4.2. Surface analysis of photolyzed thin films

Surface analysis of the photolyzed thin films was performed by Auger electron spectroscopy (AES). A photolyzed thin film of rhenium(III) pentanoate was transferred to the Ultra high vacuum (UHV) chamber of the Auger microprobe. The Auger electron spectrum was obtained at 3 keV acceleration voltage and 1.7 mA current. The spectrum showed the presence of rhenium (20%) and oxygen (54%) as the main components on the surface of the silicon chip, together with some carbon (20%). To elucidate the bulk composition of the films, a depth profile study was performed. This experiment consists in the sputtering of the film, to remove material from the surface using high-energy Ar^+ ions. After 10 s of sputtering, the carbon contamination drops below the Auger microprobe detection limit. The presence of carbon on the surface of films is commonly observed in this type of experiment and it is due to atmospheric hydrocarbon contamination, like CO_2 and low molecular weight hydrocarbons, of the surface. The AES spectrum shows the peak corresponding to Si at ∼90 keV. The peak is consistent with the observation of voids in the final photolyzed film. Because of the closeness of the main AES peaks for rhenium and chlorine, it is difficult to assign peaks in the region 160–180 keV (Re = 176 keV; Cl = 181 keV). However, the shape of the Auger peak can be used as an identification parameter. The Cl peak is always a sharp single peak. In contrast, the rhenium peak is broad and consists of three spikes, which was the case of our films. The observed peak for rhenium cor-

Table 6
AES analysis of photolyzed films of rhenium(III) carboxylates

Complexes	Sputter time (s)	%Re[a]	%O[a]	%C[a]	O/Re ratio
$Re_2(O_2C_5H_9)_4Cl_2$	0	20(±4.0)	54(±11)	26(±5.2)	2.7
	10	34(±6.8)	66(±13)	[b]	1.94
	20	49(±9.8)	51(±10)	[b]	1.04
$Re_2(O_2C_6H_{11})_4Cl_2$	0	26(±5.2)	52(±10)	22(±4.4)	2.0
	10	42(±8.4)	58(±12)	[b]	1.4
	20	47(±9.4)	53(±11)	[b]	1.1
$Re_2(O_2C_7H_{13})_4Cl_2$	0	18(±3.6)	56(±11)	26(±5.2)	3.1
	10	46(±9.2)	54(±11)	[b]	1.2
	20	39(±7.8)	61(±12)	[b]	1.56
$Re_2(O_2C_8H_{15})_4Cl_2$	0	19(±3.8)	49(±9.8)	32(±6.4)	2.6
	10	43(±8.6)	57(±11)	[b]	1.33
	20	48(±9.6)	52(±10)	[b]	1.1

[a] Error approximately 20 at%
[b] Concentration below detection limit.

Table 7
Calculated quantum yields for the decomposition of rhenium(III) carboxylates

Complexes	I_0 (mol cm^{-2} s)	ε_{UV} (cm^2 mol^{-1})	Φ_{dry}[a]	$\Phi_{ambient}$[a]
$Re_2(O_2C_5H_9)_4Cl_2$	1.95×10^{-9}	7.67×10^6	$(5.3 \pm 1.2) \times 10^{-4}$	$(4.7 \pm 0.4) \times 10^{-4}$
$Re_2(O_2C_6H_{11})_4Cl_2$	6.04×10^{-9}	4.52×10^6	$(7.5 \pm 1.4) \times 10^{-4}$	$(7.7 \pm 1.3) \times 10^{-4}$
$Re_2(O_2C_7H_{13})_4Cl_2$	1.95×10^{-9}	7.37×10^6	$(7.2 \pm 0.9) \times 10^{-4}$	$(8.4 \pm 0.05) \times 10^{-4}$
$Re_2(O_2C_8H_{15})_4Cl_2$	1.95×10^{-9}	6.79×10^6	$(4.6 \pm 0.4) \times 10^{-3}$	$(3.1 \pm 0.40) \times 10^{-3}$

[a] Error based in exponential decay fitting.

responds to a kinetic energy of 176 keV. Similar analyses were performed on thin films produced from the other rhenium(III) carboxylates. The surface of the photolyzed films showed the presence of rhenium, oxygen and carbon as surface elements. After approximately 20 s of sputtering, the carbon signal disappeared; only the peaks attributed to rhenium and oxygen were found. The Auger results are summarized in Table 6.

These results are consistent with the formation of rhenium oxide thin film after photolysis. All the photolyzed thin films followed the same trend and yielded thin films with an average atom composition of 42% Re and 58% O. The low ratio of oxygen to metal composition is a consequence of the sputtering experiment. The rate of sputtering depends on the atomic mass of the element. Oxygen is removed at a higher rate than the metal so the relative decrease of the oxygen in the bulk film is expected.

A simple X-ray photoelectron spectroscopy (XPS) was run to analyze a photolyzed thin film of rhenium(III) pentanoate. The binding energy value for the $f_{7/2}$ orbital is found at 47.4 eV (C 1s corrected) consistent with the presence of Re(VI). Broclawic et al. [7]. reported the binding energy of rhenium trioxide at 46.8 eV, indicating the presence of Re(VI) in the final film. These XPS results are consistent with the formation of ReO_3 on the final film.

5. Quantum yields

As previously described, irradiation of a thin film of rhenium(III) carboxylate led to the loss of the absorption bands associated with the starting material. Quantum yields were calculated to determine the efficiency of the photochemical reaction. The following equation was derived to describe the amount of photoreaction as function of photolysis time

$$A_t = A_0 e^{[-(2.303\varepsilon I_0 \Phi + \kappa T)t]} \quad (2)$$

In this equation, ε is the extinction coefficient (mol^{-1} cm^2) at 254 nm, I_0 is the light intensity (Einstein s), Φ is the quantum yield of the reaction, κ is the thermal decomposition rate constant (K s^{-1}) and T is the absolute temperature [18]. The quantum yields are calculated based on the decomposition reaction of the starting material.

A thin film of rhenium(III) pentanoate was formed on Si(1 0 0). The sample was irradiated with 254 nm light and the decay of the complex vibration bands over time was followed by FTIR. The absorbance intensity at 1440 cm^{-1} versus photolysis time was used to calculate the extinction coefficient.

In order to account for any effect of thermal heating of the sample during photolysis, the sample was exposed with the same source but with the lamp directed at the back side of the silicon (i.e. the non-coated face). Because of the high thermal conductivity and thickness (~300 μm) of the silicon chip used, the temperature gradient between the front and back of the substrate is assumed to be minor. Any changes in the FTIR spectrum can therefore be attributed to thermal decomposition and not to photodecomposition. This experiment showed that no changes occur in the FTIR during a similar exposure time. Therefore, the thermal coefficient in Eq. (1) can be omitted, obtaining Eq. (2).

$$A_t = A_0 e^{[-(2.303\varepsilon I_0 \Phi)t]} \quad (3)$$

The intensity of the incident 254 nm light was 1.95×10^{-9} E s^{-1} cm^{-2} and the extinction coefficient, ε_{254}, was 7.67×10^6 mol^{-1} cm^2. The quantum yields for the photodecomposition with 254-nm light, Φ_{254}, were 0.00053 ($\pm 1.2 \times 10^{-4}$) and 0.00047 ($\pm 4 \times 10^{-5}$) for dry air and ambient air experiments, respectively.

All other complexes were studied in the same manner. The photolysis was monitored by FTIR and the absorption bands due to the ligands were observed to decay over time. Plots of absorbance at 1436 ($\pm$9) cm^{-1} versus photolysis time were fit to a first order exponential decay. The experiments were repeated for all the other complexes studied when photolyzed in ambient air. The calculated quantum yields for decomposition in dry and ambient air with 254 nm light are summarized in Table 7. The calculated quantum yields are consistent with the reaction being a one-photon process and did not change when the photolysis is performed in either dry or normal air.

6. Discussion

A family of carboxylate complexes of rhenium(III) was studied on silicon surfaces. The original synthesis involved reacting tetrabutylammonium octachlorodirhenate with a mixture of the corresponding carboxylic acid and carboxylate anhydride. This approach failed in producing *n*-alkyl carboxylates with linear alkyl chain longer than 5 atoms because of the high temperature needed to activate the reaction usually higher than the decomposition temperature of the product. The alternative synthesis consisted in refluxing the rhenium(III) acetate with the minimum volume of the deoxygenated carboxylic acid, the rhenium(III) pentanoate, hexanoate, heptanoate and 2-ethylhexanoate were synthesized in this way. This approach reduced the refluxing times and increased the yields of the reaction. In addition, the compounds could be isolated by simply

cooling down the solution obtaining them highly pure. When the rhenium(III) carboxylates were spin coated on oxide coated silicon, the X-ray diffraction pattern (recorded at room temperature) exhibited a series of sharp reflections with reciprocal lattice spacing in the ratios 1:2:3, indicating that the complexes adopt a lamellar structure on the surface of the silicon substrate. The diffraction patterns were consistent with those obtained for copper(II) alkanoates [19] and praseodymium(III) alkanoates [20]. The lamellar structure of the rhenium(III) carboxylates can be described as a layered structured comprised of the polar cores (Cl–Re–Re–Cl) separated by two layers of paraffinic chains. From the X-ray data, the interlayer separations were calculated and an increase in interlayer separation of 2.5 Å, equivalent to two carbon atoms, was found. This value compares reasonably well with the value of 2.54 Å found for normal paraffin in the crystalline state. It also indicates that, in the rhenium(III) carboxylate thin film, the average direction of the chains lies at an angle of about 10° with respect to the perpendicular to the layers.

As already outlined, fabrication of metal oxides thin films by low temperature process is highly desirable. In this approach, using UV light make the process even more attractive because of the potential to be applied in energy sensitive process like the ones found in electronic industry. The calculated values of quantum yield for thin films of rhenium(III) carboxylates indicated a slow photochemical process, supporting the idea of that some recombination must be occurring in the film. This is consistent with the observation that the initial thin films showed a clear XRD pattern, i.e. crystalline films. However, it appears that the quantum yields increase with the increase in the number of carbon atoms in the alkyl chain suggesting that fragmentation products can escape the film and drive the reaction to completion. The highest calculated quantum yield was obtained for thin films of rhenium(III) 2-ethylhexanoate, the only precursor that did not show a crystalline phase ($\Phi = 0.004$). We believe that the amorphous nature of the thin films helps in the diffusion of the ligand away from the intermediate and from the film, hence facilitating the decomposition of the starting material. In all the cases, the photochemical reaction fit a first order exponential decay, which is consistent with a one-photon process. It also ruled out the occurrence of radical chain reactions that could speed up the decomposition reaction. No intermediates were observed in the FTIR supporting a single photon reaction. Mass spectra analysis of the vapor phase above the films during photolysis indicated the presence of a decarboxylation reaction (CO_2 and radical disproportionation products). This evidence suggests that during the photolysis the most probable product is rhenium metal, which is later oxidized in air to an oxide. Based on the evidence from FTIR and XRD, the formation of ReO_3 is the most probable oxide. However, from a thermodynamic point of view, Re_2O_7 ($\Delta H_f^\circ = -1273\,kJ\,mol^{-1}$) is the most stable oxide, followed by ReO_3 ($\Delta H_f^\circ = -593\,kJ\,mol^{-1}$). During the oxidation in dry air, the FTIR of the photolyzed film showed two peaks growing at approximately 940 and 840 cm^{-1}. Although the former band was assigned to the $\nu_{as}(ReO_3)$ and the later to ν_{as}(O–Re–O), the presence of both absorption bands could also be assigned to Re_2O_7. Interestingly, when left in air the bands coalescence into a single sharp peak. As already stated, the band is reminiscent of the one found in ReO_3 films formed by direct sublimation of ReO_3 onto silicon, [9] and be due to the infrared active lattice vibration of the ReO_3 crystal. The observed FTIR frequencies of ReO_3 when compared with those of WO_3 and Re_2O_7 indicated that the metal oxygen bond vibrations are essentially the same as the insulating WO_3 and Re_2O_7. So the FTIR evidence is not conclusive to assume the formation of one rhenium oxide in particular. However, the observation of a clear XRD pattern in photolyzed thin films is more conclusive in the formation of rhenium trioxide as main product of photolysis. Further evidence comes from XRD studies of samples exposed to air for longer period of time. Although ReO_3 is generally described as a chemically stable compound in air at room temperature, a series of XRD studies [21,22] have revealed that the crystal readily reacts with water vapor to form a new phase, a cubic rhenium oxide bronze, which is also denoted as H_xReO_3. The changes observed in the XRD pattern for the photolyzed thin films are consistent with the formation of a H_xReO_3 ($x = 0.57$) phase and support the assumption of ReO_3 being the initial product of photolysis, product that later react with moisture to produce H_xReO_3 and $HReO_4$, with the later being a liquid at room temperature.

7. Conclusions

The photochemistry of rhenium(III) carboxylates was studied as thin films on silicon. The synthesized and characterized rhenium(III) carboxylates showed mesomorphic behavior when deposited as thin films on silicon dioxide. Close structural similarities to other bimetal carboxylate complexes (like copper(II) carboxylates) were found. The rhenium(III) pentanoate and longer chain carboxylates were found to form lamellar bilayer structures on silicon dioxide by spin coating where planes of rhenium(III) are separated by the carboxylates alkyl chains. The interlayer separation was found to be proportional to the number of carbons in the alkyl chain, in close agreement with the values of paraffinic bilayers. The photolysis of these complexes led to the formation of ReO_3. Because of the moisture sensitivity and FTIR evidence, the photolysis in dry air yields thin films consisting of rhenium trioxide, although some presence of rhenium heptoxide could not be ruled out. The thin films produced reacted over time with moisture in the air to induce a new phase consistent with the formation of a rhenium bronze structure (H_xReO_3). Attempt to measure conductivity was not conclusive, due to the powdery nature of the films some areas of the film showed some conductivity but experiments were difficult to repeat consistently. However, approaches to deposit metal oxides like the one described in this paper is promising as a low temperature process for applications in thermal sensitive devices. Also, rhenium(III) carboxylates of longer alkyl chains are good candidates for the synthesis of new types of rhenium containing metallomesogens.

Acknowledgements

This work was financed by a grant by National Science Engineering Research Council (NSERC) Canada and with the

additional support of EKC DuPont Technologies, Hayward, CA, USA.

References

[1] A.P. Ketteringham, C. Oldham, C.J. Peacock, J. Chem. Soc. Dalton Trans, Inorg. Chem. (1972–1999) (1976) 1640–1642.
[2] S. Ye, W.K. Leong, J. Organometall. Chem. 691 (2006) 1216–1222.
[3] H. Miyazaki, I. Yasui, Appl. Surf. Sci. 252 (2006) 8367–8370.
[4] V. Shrotriya, G. Li, Y. Yao, C.-W. Chu, Y. Yang, Appl. Phys. Lett. 88 (2006), 073508/073501-073508/073503.
[5] K.L. Jiao, L.H. Chang, R. Wallace, W.A. Anderson, Appl. Superconductivity 3 (1995) 55–60.
[6] M.A. lunell S, P.L. Alemany, J. Chem. Soc., Dalton Trans. (1998) 1195.
[7] E. Broclawik, J. Haber, L. Ungier, J. Phys. Chem. Solids 42 (1981) 203–208.
[8] M. Ohkubo, K. Fukai, M. Kohji, N. Iwata, H. Yamamoto, Superconductor Sci. Technol. 15 (2002) 1778–1780.
[9] M. Ishii, T. Tanaka, T. Akahane, N. Tsuda, J. Phys. Soc. Jpn. 41 (1976) 908–912.
[10] M.G. Khrisna, A.K. Mhattacharya, Solid State Commun. 116 (2000) 637.
[11] A.A. Avey, R.H. Hill, J. Am. Chem. Soc. 118 (1996) 237.
[12] F.A. Cotton, C. Oldham, W.R. Robinson, Inorg. Chem. 5 (1966) 1798–1802.
[13] D.S. Martin, R.A. Newman, L.M. Vlasnik, Inorg. Chem. 19 (1980) 3404–3407.
[14] C.M. Kennedy, T.C. Pinkerton, Appl. Radiat. Isotopes 39 (1988) 1159–1165.
[15] I.R. Beattie, T.R. Gilson, P.J. Jones, Inorg. Chem. 35 (1996) 1301–1304.
[16] T.I. Dyuzheva, N.A. Bendeliani, S.S. Kabalkina, J. Less Common Met. 133 (1987) 313–317.
[17] C.A. Majid, M.A. Hussain, J. Phys. Chem. Solids 56 (1995) 255–259.
[18] J.P. Bravo-vasquez, R.H. Hill, J. Photochem. Photobiol. A: Chem. 193 (2007).
[19] H. Abied, D. Guillon, A. Skoulios, P. Weber, A.M. Giroud-Godquin, J.C. Marchon, Liquid Cryst. 2 (1987) 269–279.
[20] L. Jongen, K. Binnemans, D. Hinz, G. Meyer, Liquid Cryst. 28 (2001) 819–825.
[21] P.G. Dickens, M.T. Weller, J. Solid State Chem. 48 (1983) 407–411.
[22] S. Horiuchi, N. Kimizuka, A. Yamamoto, Nature (London, United Kingdom) 279 (1979) 226–227.
[23] H.J. Emeleus, A.G. Sharpe (Eds.), Advances in Inorganic Chemistry and Radiochemistry, vol. 20, 1977, p. 1977.
[24] J. Skowronek, W. Preetz, Zeitschrift fuer Naturforschung, B: Chem. Sci. 47 (1992) 482–490.
[25] D.S. Martin, H.W. Huang, R.A. Newman, Inorg. Chem. 23 (1984) 699–701.